Science Advances
AAAS

Supplementary Materials for

CBP and Gcn5 drive zygotic genome activation independently of their catalytic activity

Filippo Ciabrelli *et al.*

Corresponding author: Nicola Iovino, iovino@ie-freiburg.mpg.de

Sci. Adv. **9**, eadf2687 (2023)
DOI: 10.1126/sciadv.adf2687

This PDF file includes:

Supplementary Figure 1

A

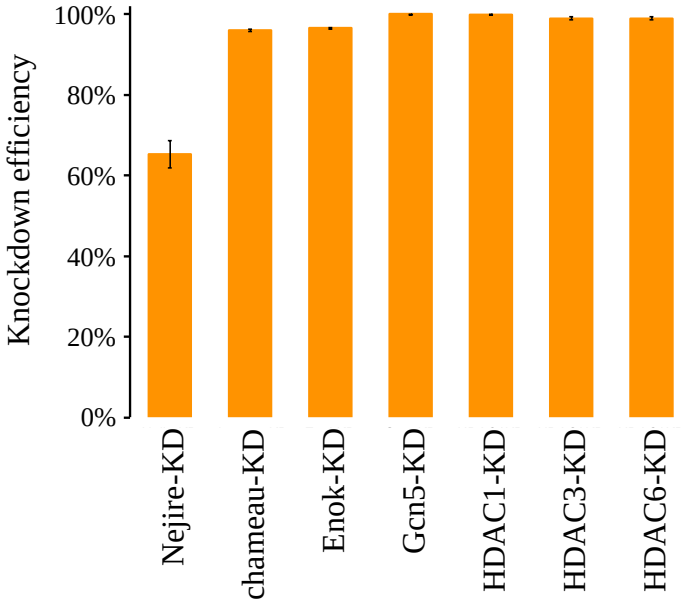

B

Gene	Name line	ID line	Type	CR	HR	PCLR
nejire	shRNA line 1	homemade	V20	35.0%	0.0%	100.0%
nejire	shRNA line 2	BL36682	V20	44.0%	0.0%	100.0%
CONTROL	control	BL36303	-	98.0%	95.0%	3.1%

C

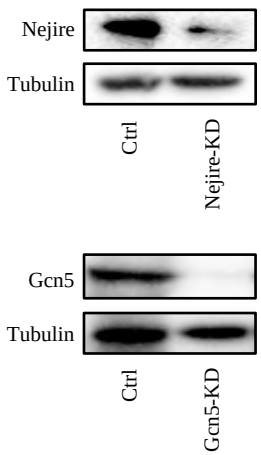

D

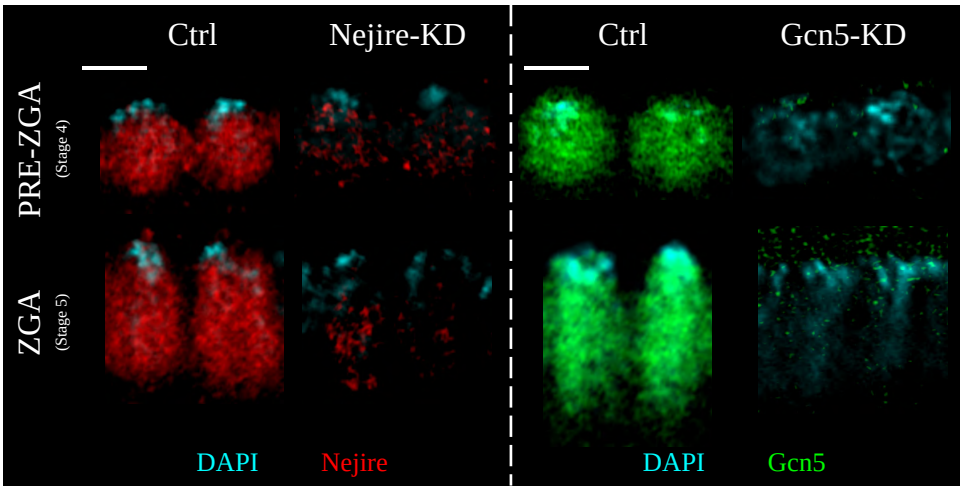

E

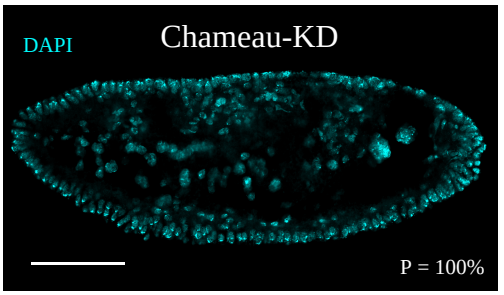

F

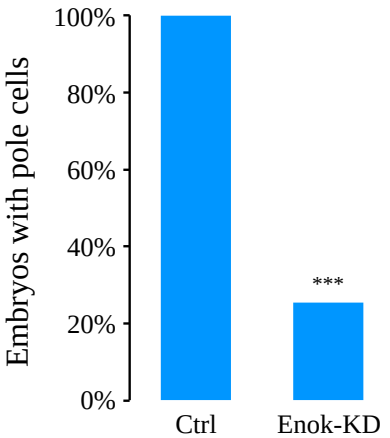

Fig. S1. Knockdown efficiency and additional embryonic phenotypes upon maternal depletion. (**A**) Knockdown efficiency of RNAi targets. Values correspond to the mean and error bar represent the standard deviation of RT-qPCR from n = 3 biological replicates of independent embryo collections at ZGA. Values are calculated subtracting from 100% the relative level of target mRNA, normalized to RP49 mRNA levels, in a given knockdown compared to the control. (**B**) Cellularization rate (CR), hatching rate (HR) and post cellularization lethality rate (PCLR) of two Nejire shRNA lines and control. (**C**) Western blot assays performed with total protein extracts from PRE-ZGA embryos (stage 4). On the top, anti-Nejire and anti-Tubulin signals are compared in control and Nejire-KD extracts. On the bottom, anti-Gcn5 and anti-Tubulin signals are compared in control and Gcn5-KD. (**D**) Representative immunofluorescence pictures of PRE-ZGA (stage 4) (top) and ZGA (stage 5) (bottom) control and knockdown embryos. On the left, anti-Nejire staining (red) and on the right, anti-Gcn5 staining (green), are coupled with DAPI staining (cyan). (scale bar = 5 µm). (**E**) DAPI staining of representative Chameau knockdown embryo at ZGA. Scale bar = 100 µm. Penetrance (P) indicates the frequency of observed embryos displaying abnormal phenotype. (**F**) Percentage of embryos displaying pole cells in control embryos (n = 47) and in Enok-KD embryos (n = 51) at ZGA. Fisher's exact test *t*-test *** *p*-value ≤ 0.001.

Supplementary Data Figure 2

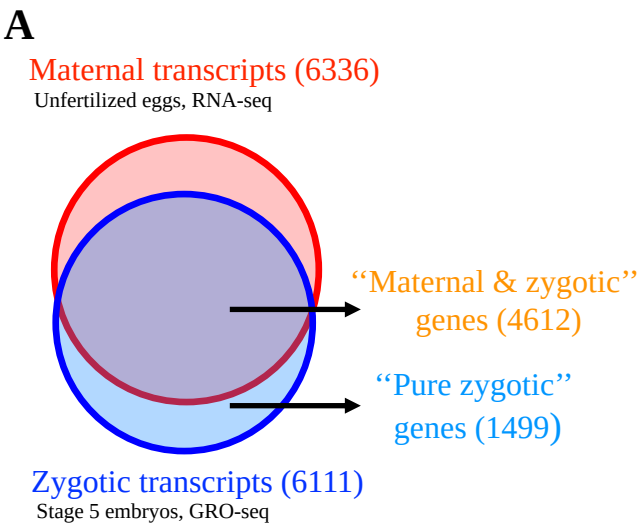

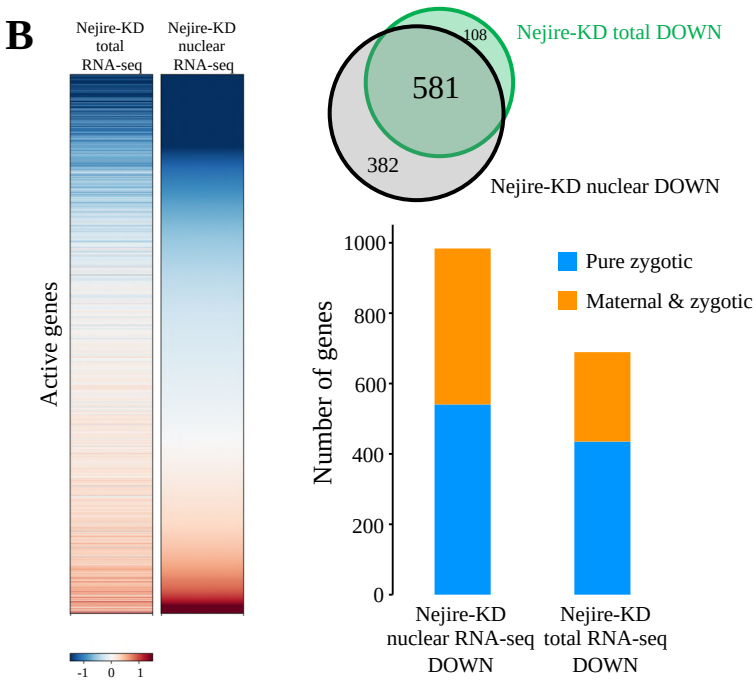

C

Nejire and Gcn5 shared downregulated genes

Symbol	Zelda-depenent	GO_BIOLOGICAL_PROCESS
Cyp312a1	yes	-
DIP-eta	yes	synapse organization
CG11905		-
Adgf-A2		inosine biosynthetic process
Art2	yes	peptidyl-arginine methylation
Rab26		regulation of exocytosis
Cad99C	yes	cell-cell adhesion
dpr1		synapse organization
Notum	yes	Wnt signaling pathway
hbs		myoblast fusion
zen2	yes	regulation of transcription by RNA polymerase II
mas	yes	axon development
lov	yes	gravitaxis
Neu2	yes	regulation of transcription by RNA polymerase II
RyR		calcium ion transport
tld	yes	BMP signaling pathway
scw	yes	BMP signaling pathway
CG6885	yes	-
geko	yes	behavioral response to ethanol
saturn		-
Rpi		D-ribose metabolic process
CG13716	yes	regulation of localization
Mco1	yes	iron ion transport
CG16813	yes	-
CG1146	yes	-
CG7271	yes	-
Ldh		carbohydrate metabolic process
Elba3	yes	heterochromatin boundary formation
fd96Cb		Regulation of transcription by RNA polymerase II
pyd3		pyrimidine nucleobase catabolic process
srw	yes	BMP signaling pathway
CG13712	yes	regulation of localization
CG14317	yes	proteolysis
sc	yes	central nervous system development
Obp99a	yes	response to pheromone
zen	yes	regulation of transcription by RNA polymerase II
ND-51L1	yes	mitochondrial electron transport
tsg	yes	BMP signaling pathway
dunk	yes	syncytial embryo cellularization
upd1	yes	JAK-STAT pathway
Bro	yes	regulation of transcription by RNA polymerase II
nej		histone acetylation
CG9775	yes	-
Tep2		innate immune response
alpha-Est1		-
amos	yes	dendrite morphogenesis
D		dorsal/ventral axis specification
CG13713	yes	regulation of localization
Cyp6a20		defense response to Gram-negative bacterium
CG11034		proteolysis
ph-d		negative regulation of transcription
spri	yes	signal transduction

34/52
Zelda-dependent

D

Pre-ZGA

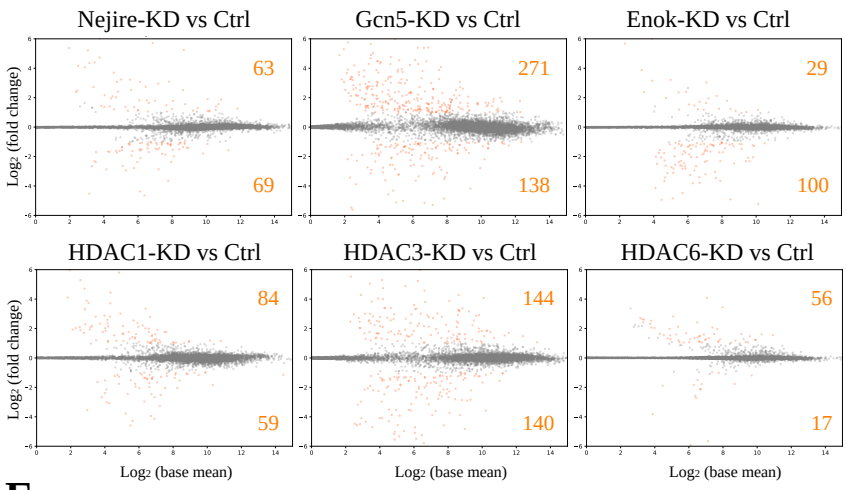

E

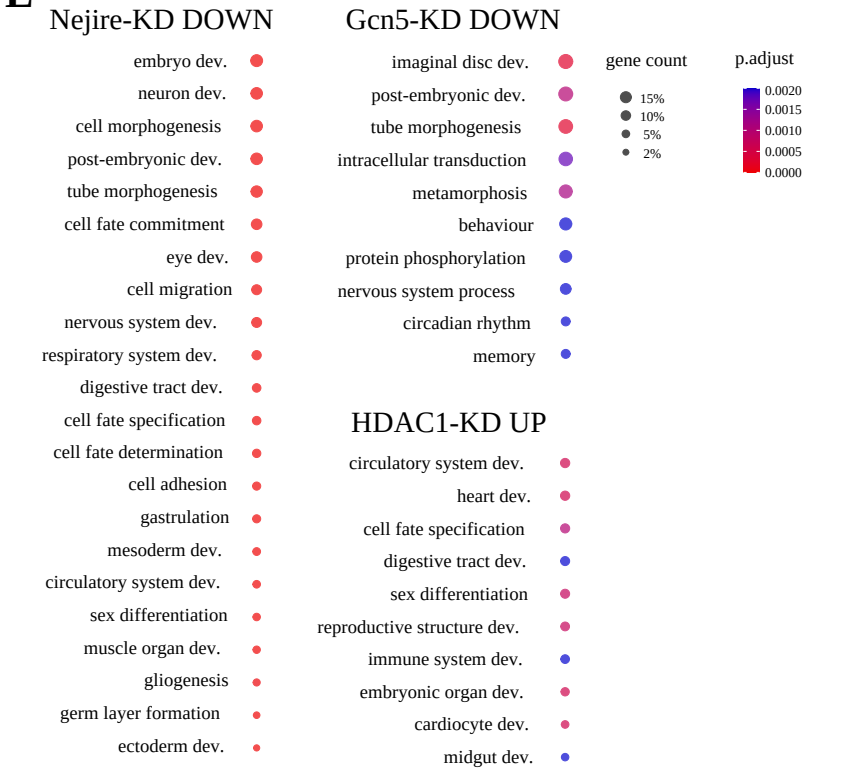

Fig. S2. HATs and HDACs regulate different sets of genes during ZGA. (**A**) **"**Maternal & Zygotic" and "Pure Zygotic" gene-classification based on the overlap between "Zygotic transcripts" (Genes displaying GRO-seq signal at ZGA (*15*) also defined as "active genes") and "Maternal genes" (RNA-seq positive genes in unfertilized eggs (*15*)). In parenthesis the numbers of transcripts/genes for each category. (**B**) Comparison between total RNA-seq and nuclear RNA-seq between Nejire-KD and control at ZGA. On the left, a heatmap displaying the change in gene expression between Nejire-KD and control among active genes, ranked by the Nuclear RNA-seq wt/-KD ratio. Corresponding log2FC color-coded scale bars are depicted on the bottom. On the top right, Venn diagram displaying the overlap between the number of active genes significantly downregulated in Nejire-KD (adjusted *p*-value ≤ 0.05 and log2FC < -1) in total RNA-seq (green) and the number of active genes significantly downregulated in Nejire-KD (adjusted *p*-value ≤ 0.05 and log2FC < -1) in nuclear RNA-seq (black). On the bottom right, number of "Pure Zygotic" (blue) and "Maternal & Zygotic" (orange) genes (see fig. S2A for details) significantly downregulated in nuclear RNA-seq and total RNA-seq in Nejire-KD. (**C**) List of 52 overlapping genes between Nejire-dependent and Gcn5-dependent active genes at ZGA (adjusted *p*-value ≤ 0.05 and log2FC < -1). Column 2 shows Zelda dependency (see (*15*) for details) and column 3 shows GO biological process. (**D**) MA plots displaying total RNA-seq experiments performed on Pre-ZGA (stage 2) embryos, comparing knockdown with Ctrl. Significantly misregulated genes (adjusted *p*-value ≤ 0.05 and log2FC < -1 or log2FC > 1) are highlighted in orange. The numbers of significantly upregulated or down regulated genes are shown above or below the log2FC mean expression = 0 line, respectively. (n = 2 biological replicates from independent embryo collections). **e**, Top GO terms are shown for HDAC1-KD upregulated (adjusted *p*-value ≤ 0.05 and log2FC > 1) and Nejire or Gcn5 downregulated (adjusted *p*-value ≤ 0.05 and log2FC < -1) active genes at ZGA. For each term, color intensity represents the adjusted *p*-value and dot size shows the number of genes which support the corresponding GO term.

Supplementary Data Figure 3

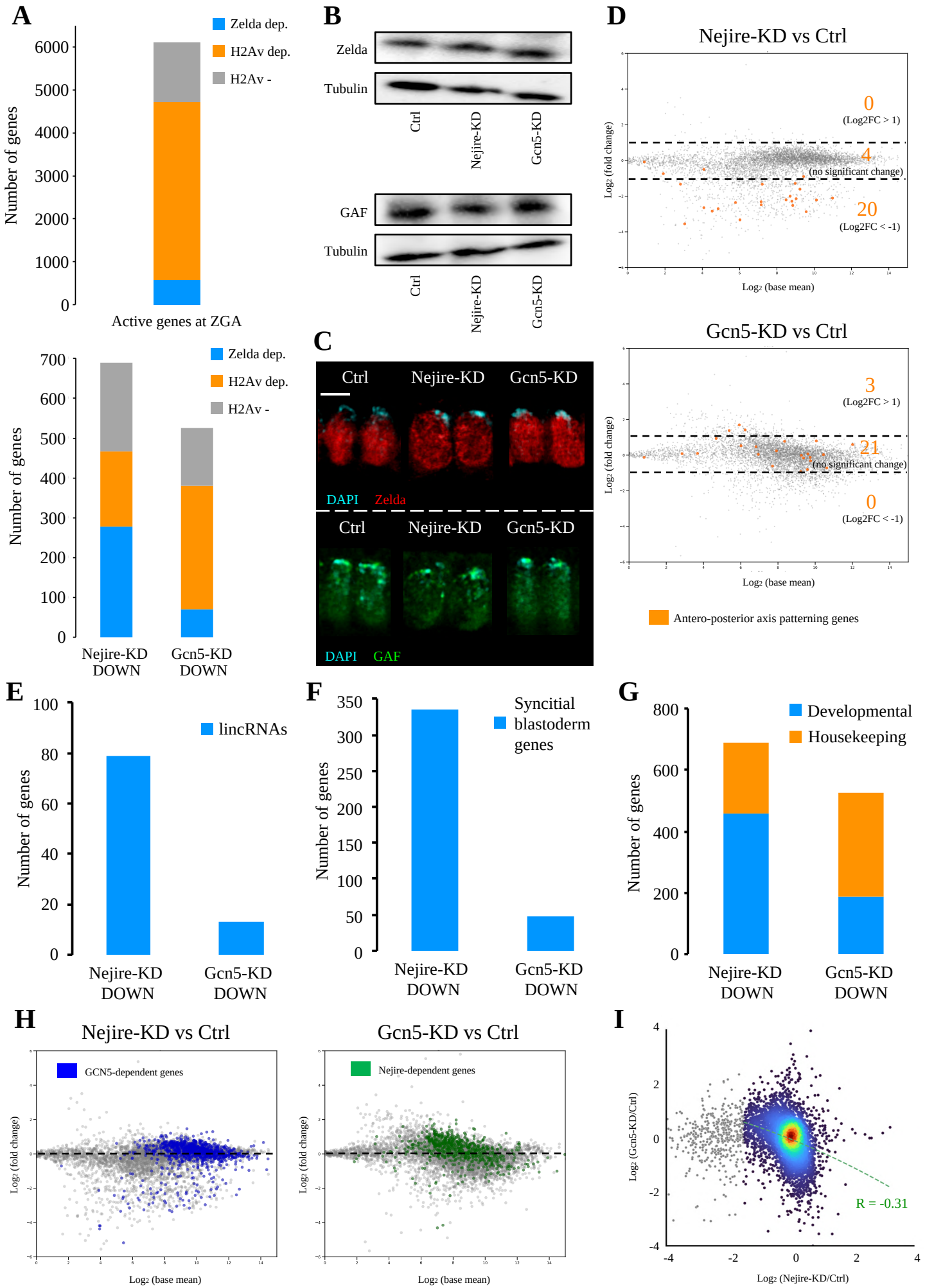

Fig. S3. Nejire and Gcn5 regulate the expression of different sets of genes during ZGA. (**A**) On the top, the number of Zelda-dependent ("Zelda dep.", in blue), H2Av-dependent ("H2Av dep.", in orange) and Zelda-independent/H2Av-independent ("H2Av –", in grey) active genes (see ref. (*15*) for details) at ZGA. On the bottom, the Zelda/H2Av categorization applied to the genes significantly downregulated in total RNA-seq in Nejire-KD and in Gcn5-KD (adjusted *p*-value ≤ 0.05 and log2FC < -1). (**B**) Western blot assays performed with total protein extracts from PRE-ZGA embryos (stage 4). On the top, anti-Zelda and anti-Tubulin, on the bottom, anti-GAF and anti-Tubulin signals are compared in control and Nejire-KD and Gcn5-KD embryonic extracts. (**C**) Representative immunofluorescence pictures of ZGA control, Nejire-KD and Gcn5-KD and knockdown embryos. On the top, anti-Zelda staining (red) and on the bottom, anti-GAF staining (green), are coupled with DAPI staining (cyan). (scale bar = 5 µm). (**D**) MA plots displaying total RNA-seq experiments, comparing Nejire-KD (top) and Gcn5-KD (bottom) with Ctrl at ZGA. Highlighted in orange 24 early antero-posterior axis patterning genes (trunk gap genes, pair-rule genes, segment polarity genes and homeotic genes). Numbers indicate significantly upregulated, downregulated (adjusted *p*-value ≤ 0.05 and log2FC < -1 or log2FC > 1), and the not significantly affected among the 24 considered genes. (**E**) Number of lincRNA genes significantly downregulated (adjusted *p*-value ≤ 0.05 and log2FC < -1) in Nejire-KD and Gcn5-KD compared to Ctrl at ZGA. (**F**) Number of "Syncytial blastoderm" expressed genes significantly downregulated in Nejire-KD and Gcn5-KD (adjusted *p*-value ≤ 0.05 and log2FC < -1) among the 510 genes still expressed at ZGA. (see (*15*) and (*8*) for details). (**G**) Number of "Developmental" (blue) and "Housekeeping" (orange) genes significantly downregulated (adjusted *p*-value ≤ 0.05 and log2FC < -1) in Nejire-KD and Gcn5-KD at ZGA. Genes are defined as "Housekeeping" when their expression is higher than the 40th percentile in each of the 30 distinct developmental conditions tested in modEncode RNA-Seq (*81*). All the other genes are considered as "Developmental". (**H**) MA plots of total RNA-seq experiments, comparing Nejire knockdown (left) and Gcn5 knockdown (right) with Ctrl embryos at ZGA. Only active genes are displayed (see fig. S2A and ref. (*15*) for details). In blue, significantly downregulated genes (adjusted *p*-value ≤ 0.05 and log2FC < -1) in Gcn5-KD are overlaid in the Nejire-KD vs Ctrl MA plot on the left. In green, significantly downregulated genes (adjusted *p*-value ≤ 0.05 and log2FC < -1) in Nejire-KD are overlaid in the Gcn5-KD vs Ctrl MA plot on the right. (**I**), Scatter plot displaying active genes log2FC in Nejire-KD (x-axis) versus Gcn5-KD (y-axis) at ZGA. Strong Nejire targets (log2FC < -1.5 in Nejire-KD) are highlighted in grey. Dashed green trendline shows the anticorrelation (R = -0.31) between Nejire-KD and Gcn5-KD of the fold change in gene expression among the rest of active genes (log2FC > -1.5 in Nejire-KD).

Supplementary Data Figure 4

A

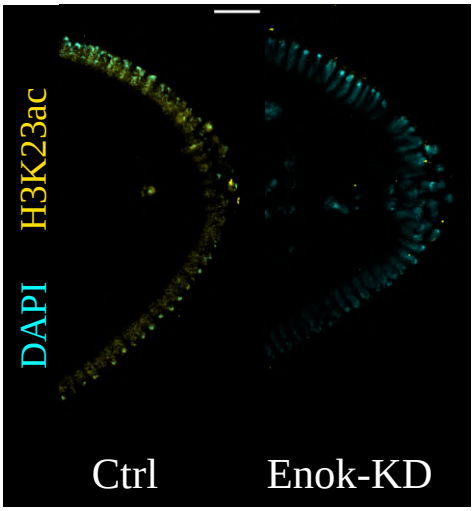

B

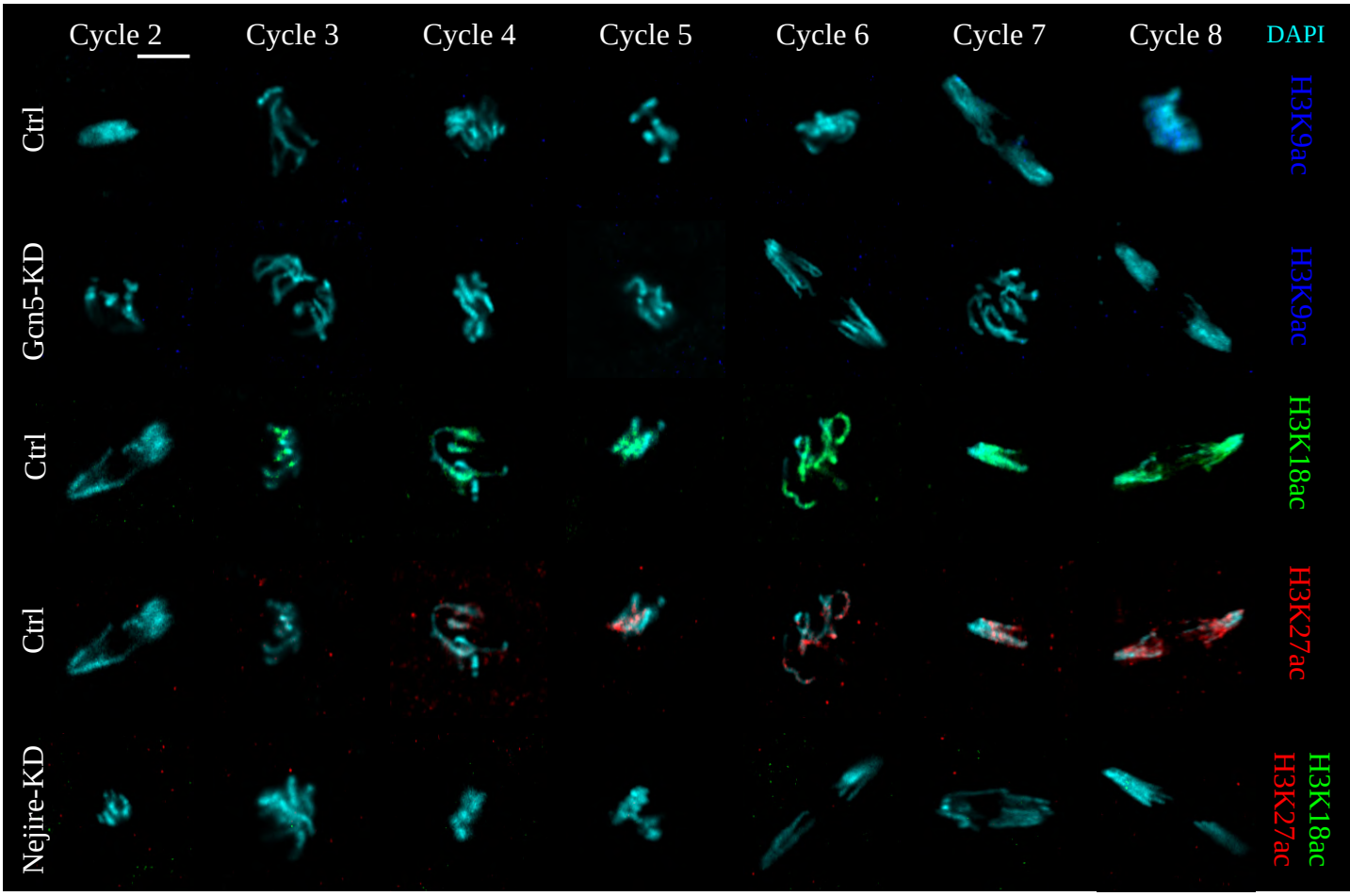

Fig. S4. H3K9-, H3K18- and H3K27ac deposition precede the first wave of ZGA. (**A**) Representative pictures of posterior side control embryo (left) and Enok-KD embryo (right) stained with anti-H3K23ac (yellow), and DAPI (cyan) at ZGA. Scale bar = 20 µm. (**B**) Representative pictures of mitotic nuclei from cycle 2 to cycle 8 of embryogenesis (scale bar = 5 µm). On the top, control embryos and Gcn5-KD embryos stained with anti-H3K9ac (blue) and DAPI (cyan). On the bottom, control embryos stained with anti-H3K18ac (green) and DAPI; control embryos stained with anti-H3K27ac (red) and DAPI (cyan); Nejire-KD embryos stained with anti-H3K18ac (green), anti-H3K27ac (red) and DAPI (cyan).

Supplementary Data Figure 5

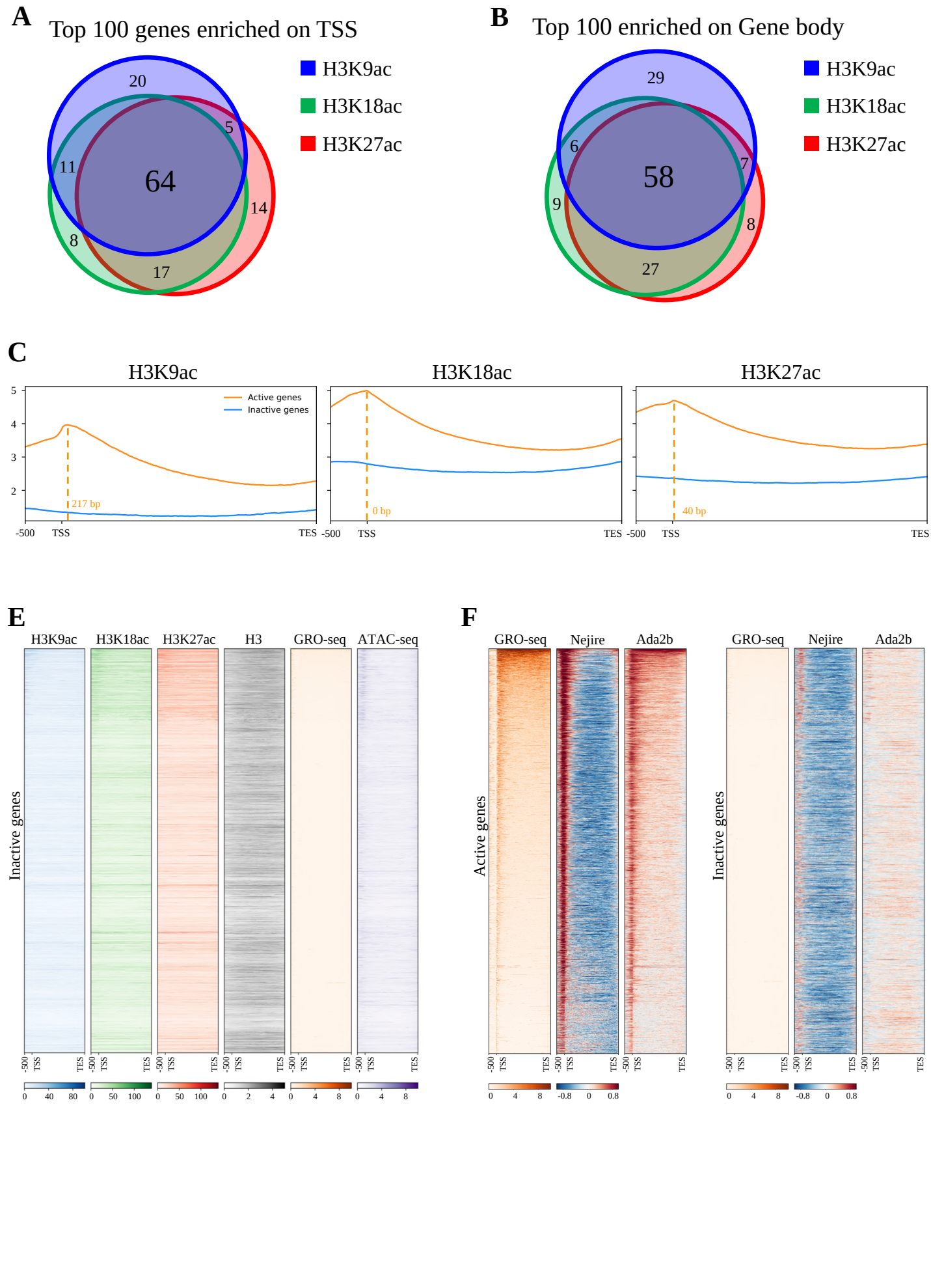

Fig. S5. H3K9-, H3K18- and H3K27ac marks and their writers are specifically deposited on active genes. (**A** and **B**) Venn diagram displaying the overlap among the top 100 active genes enriched for H3K9ac (blue), H3K18ac (green) and H3K27ac (red) marks, normalized by total H3 levels, in the genomic region spanning around their TSS (200 bp upstream TSS to 200 bp upstream TSS) (A) **or** on their gene body (from 200 bp downstream of TSS to TES) (B). (**C**) Metagene profiles of H3 normalized H3K9ac (left), H3K18ac (center) and H3K27ac (right) marks, showing active genes (orange) and inactive genes (blue) at ZGA from 500 bp upstream the TSS to TES. Numbers in orange indicate the distance from the TSS to the peak. Numbers on Y-axis indicate the mean coverage of log2 of the corresponding H3 normalized acetylation marks. (**D**) Heatmaps of ZGA (stage 5) inactive genes defined by lack of a GRO-seq and PolII signals spanning from 500 bp upstream of TSS to TES. Genes are ranked according to their GRO-seq signal in column 5 (orange). Columns represent wild-type embryos H3K9ac CUT&Tag (blue), H3K18ac CUT&Tag (green), H3K27ac CUT&Tag (red), H3 CUT&Tag (grey), GRO-seq (orange), ATAC-seq (purple) (*15*). Corresponding color-coded scale bars are depicted on the bottom (n = 2 biological replicates from independent embryo collections). (**E**) Heatmaps of active genes (left) and inactive genes (right) spanning from 500 bp upstream of TSS to TES during ZGA. Genes are ranked according to their GRO-seq signal in column 1 (orange). Columns 2 shows Nejire ChIP signal from (*48*). Column 3 shows Ada2b signal (SAGA component) from (*35*). Corresponding color-coded scale bars are depicted on the bottom (n = 2 biological replicates from independent embryo collections).

Supplementary Data Figure 6

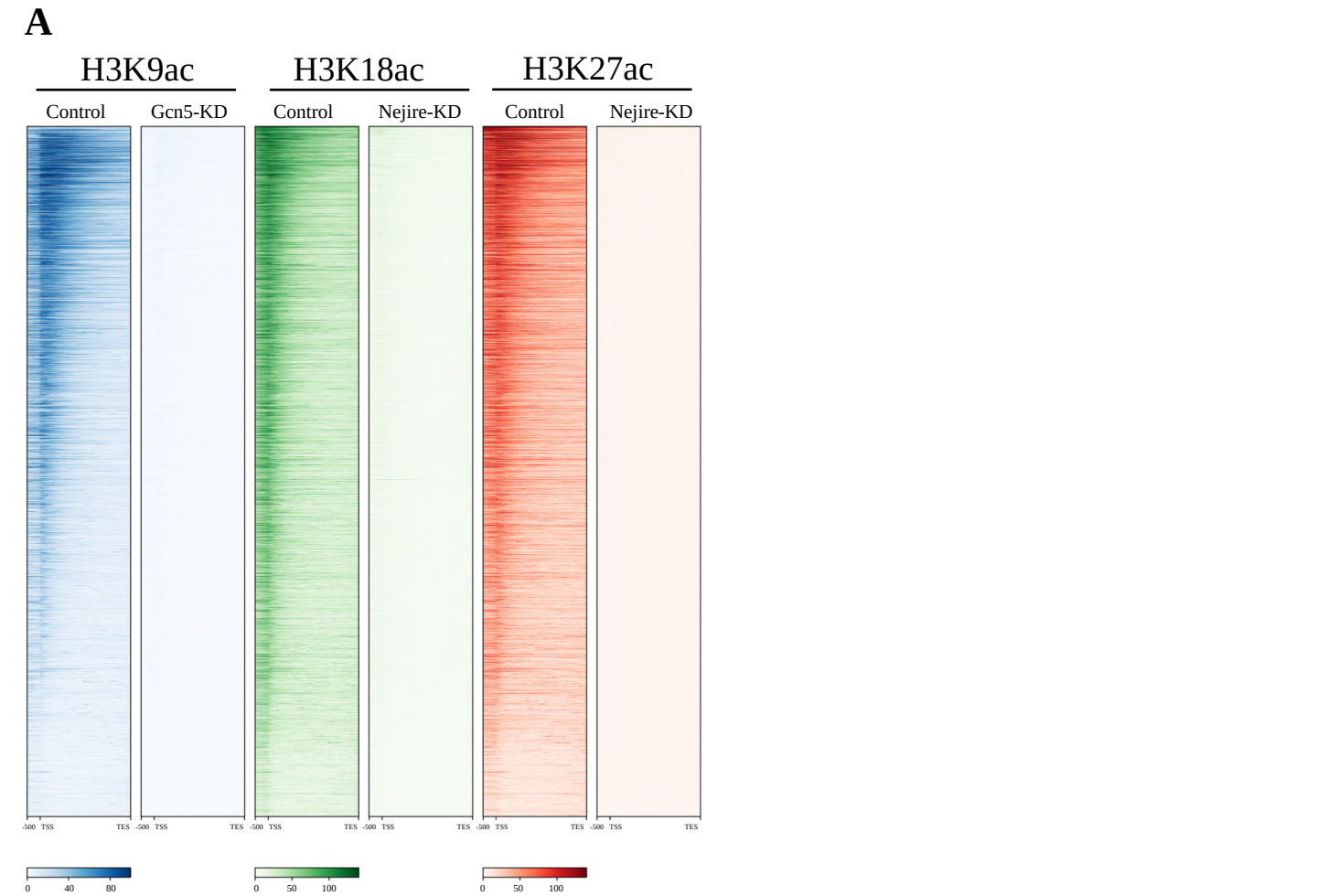

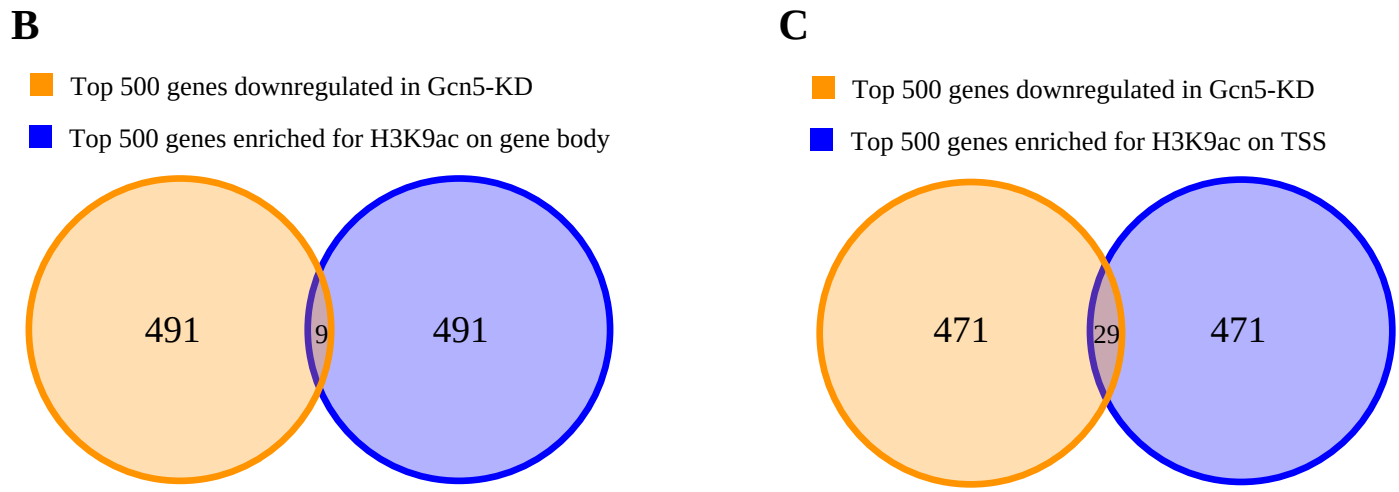

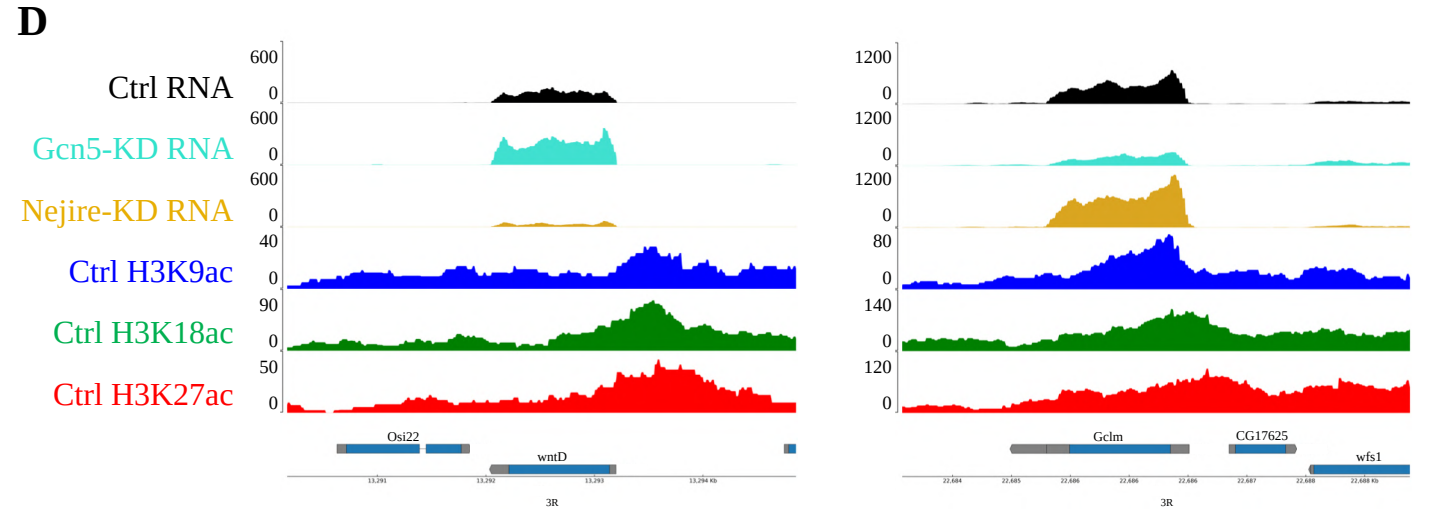

Fig. S6. Nejire and Gcn5 deposit their acetylation marks on every active gene, independently of their transcriptional coactivator activities. (**A**) Heatmaps of ZGA (stage 5) active genes defined by a GRO-seq signal (*15*) spanning from 500 bp upstream of TSS to TES. H3K9ac (blue), H3K18ac (green) and H3K27ac (red) marks are shown in control embryos on the left and in their corresponding knockdown on the right. Corresponding color-coded scale bars are depicted on the bottom (n = 2 biological replicates from independent embryo collections). (**B and C**) Venn diagram displaying the overlap among the top 500 genes enriched for H3K9ac mark normalized by total H3 (blue) on their gene body (from 200 bp downstream of TSS to TES) (B) or on their TSS (200 bp upstream TSS to 200 bp upstream TSS) (C) with the top 500 genes downregulated in Gcn5-KD compared to control in RNA-seq experiments during ZGA. (**D**) IGV gene browser views of a representative Nejire-dependent gene (*wntD*) on the left and a representative Gcn5-dependent gene (*Gclm*) on the right. For each genomic region, control RNA-seq (black), Gcn5-KD RNA-seq (cyan), Nejire-KD RNA-seq (gold), H3K9ac (blue), H3K18ac (green), and H3K27ac (red) CUT&Tag are displayed from top to bottom. Genomic coordinates are indicated above the panel.

Supplementary Data Figure 7

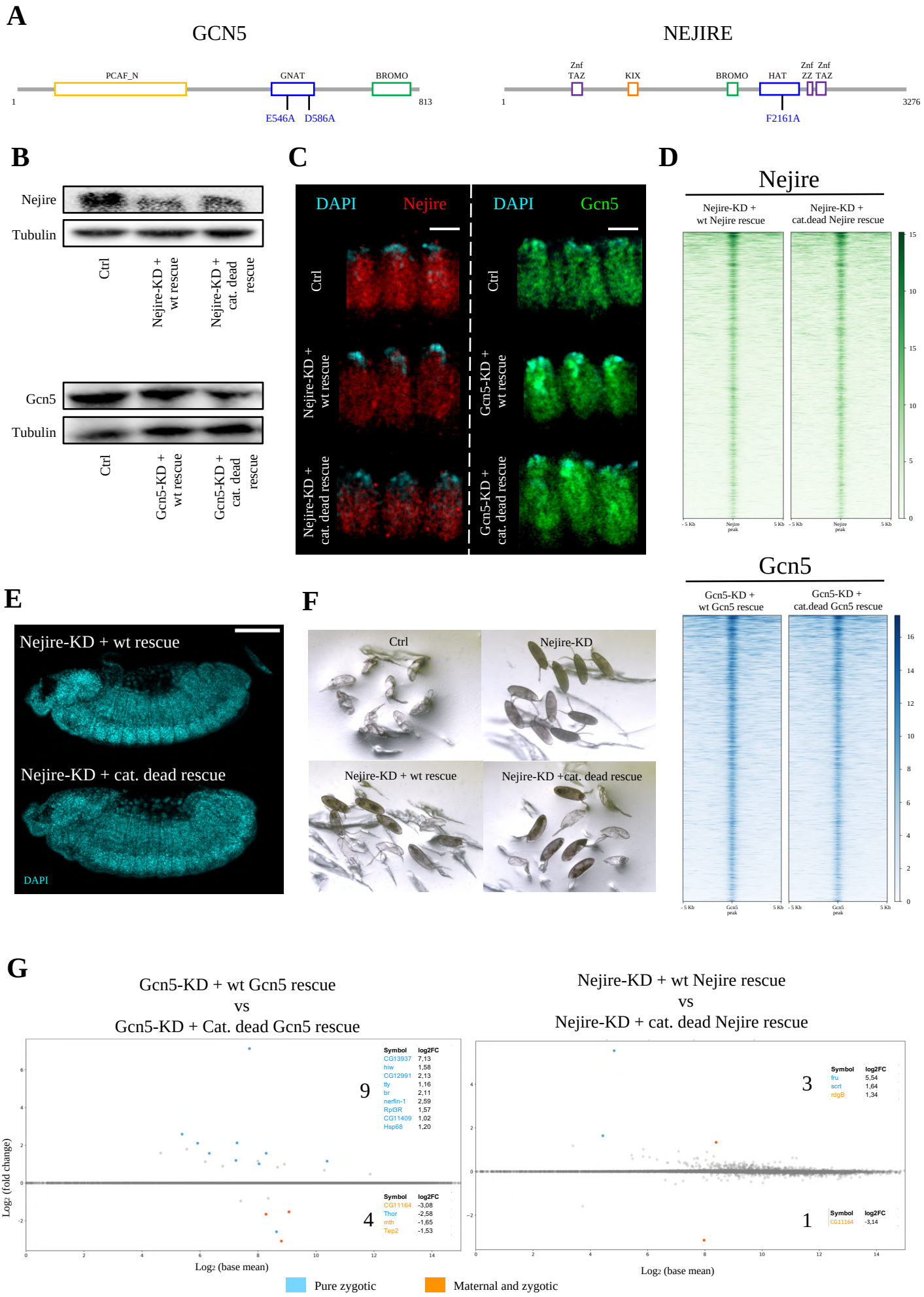

Fig. S7. Nejire and Gcn5 catalytic activities are not required for embryonic development. (**A**) Representation of Gcn5 and Nejire protein products with their corresponding domains. Numbers indicate aminoacidic positions. In blue, the aminoacidic substitutions in the catalytically dead constructs within the HAT domains. (**B**) Western blot assays performed with total protein extracts from ZGA embryos. On the top, anti-Nejire and anti-Tubulin, on the bottom, anti-Gcn5 and anti-tubulin signals are compared in control, wild-type rescue and catalytically dead rescue embryonic extracts. (**C**) Representative immunofluorescence pictures of ZGA embryos. On the left, anti-Nejire staining (red) and on the right, anti-Gcn5 staining (green), are coupled with DAPI staining (cyan). (scale bar = 5 µm). (**D**) Heatmaps of ZGA CUT&Tag experiments performed in ZGA embryos, comparing wild type rescue and on the left and catalytically dead rescues on the right of Nejire-KD (top) and Gcn5-KD (bottom), respectively. Signal span 5 Kb upstream and 5 Kb downstream of Nejire peaks (green) on the top and Gcn5 peaks (blue) on the bottom. Corresponding color-coded scale bars are depicted on the bottom (n = 3 biological replicates from independent embryo collections) (**E**) DAPI staining of representative embryos during the beginning of dorsal closure (stage 14). Nejire-KD embryos coupled on the left with wild-type Nejire rescue or with Nejire catalytically dead rescue on the right. Scale bar = 100 µm. (**F**) Pictures of holocarbon oil-immersed embryos, 25 hours after egg deposition in the corresponding conditions. Empty cases correspond to hatched embryos. Abdominal segments are visible in embryos that died at late stages of embryogenesis (**G**) MA plots of RNA-seq experiments from total RNA in ZGA embryos, comparing the indicated conditions. The number of significantly upregulated and downregulated genes (adjusted *p*-value ≤ 0.05 and log2 FC < -1 or log2FC > 1) is shown above or below the log2FC mean expression = 0 line, respectively. The affected genes are listed on the right and they are highlighted in blue if “pure zygotic” or in orange if “maternal and zygotic” (see fig. S2A for details on classification).

Supplementary Data Figure 8

A

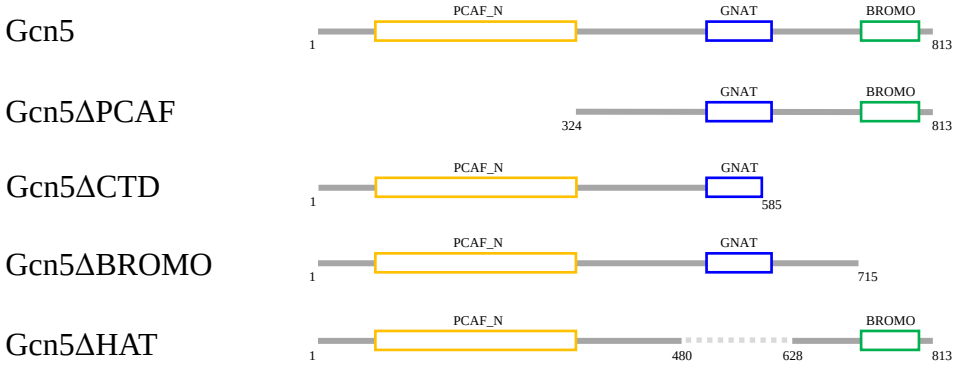

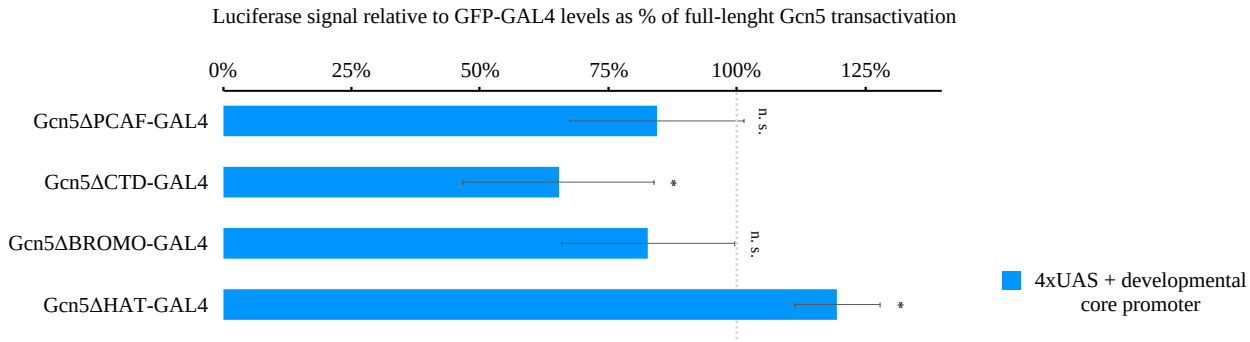

B

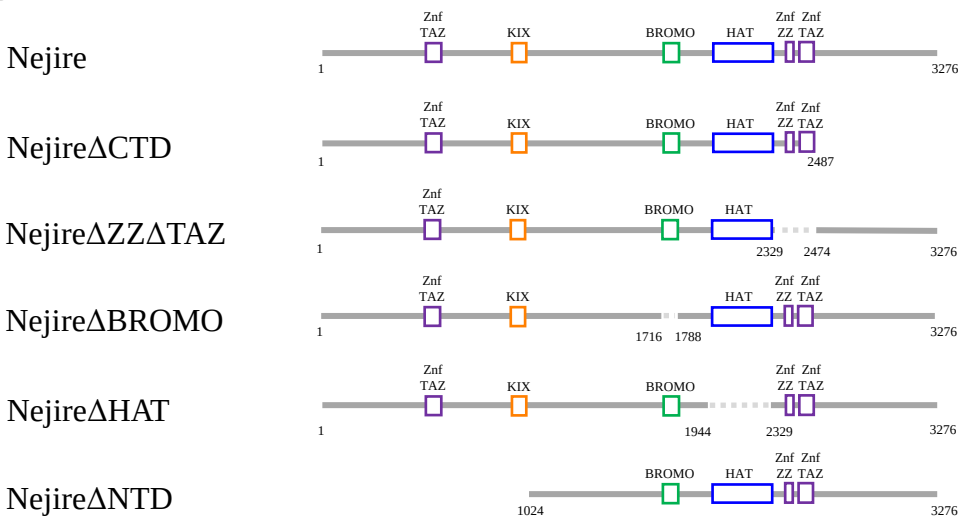

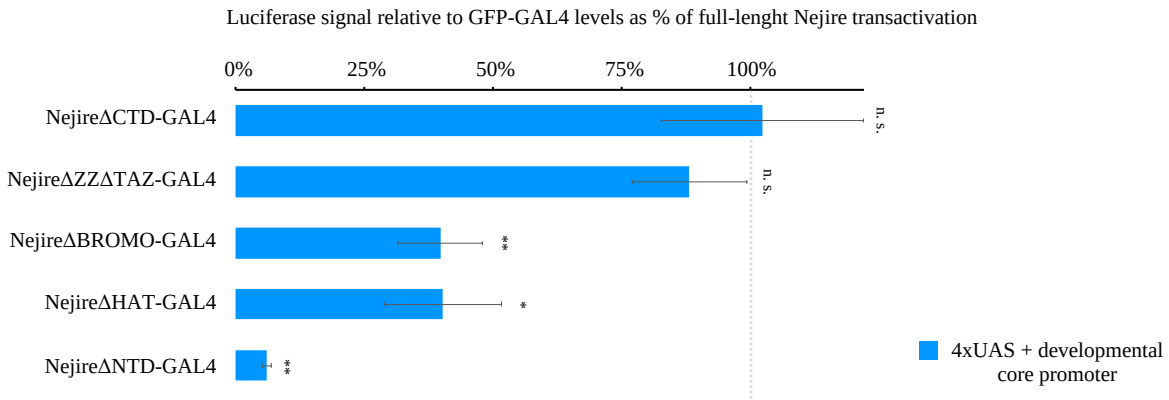

Fig. S8. Nejire N-terminal domain is crucial for *in vitro* transactivation. (**A,B**) On the top, Gcn5 (**A**) and Nejire (**B**) schematics of truncated protein variants. Numbers represent aminoacidic position is full-length protein. Domains are highlighted in colors. On the bottom, the results of *firefly* luciferase transactivation assay upon the recruitment of Gcn5 variants (**A**) and Nejire variants (**B**), using a developmental core promoter. The *firefly* luciferase signal is normalized to the *renilla* luciferase signal expressed from a constitutive promoter to control for transfection efficiency. Signals are further normalized to GFP-GAL4DBD as negative control. Finally, the relative GFP for each transfection replicate is normalized to full-length Gcn5 (**A**) or Nejire (**B**) transactivation levels. For each independent transfection replicate, three technical measurement replicates were averaged. Data are represented as mean and standard deviation of n = 4 transfection replicates. Paired, two-tailed Student's *t*-Test was applied to compare the GFP-GAL4DBD relative *firefly*/*renilla* luciferase levels with the other conditions (* p-value ≤ 0.05, ** p-value ≤ 0.01, *** p-value ≤ 0.001).

Table S1. Screen results of maternal knockdown of chromatin factor

#	Symbol	ID line	Type	CR	HR	PCLR	Eggs	Category
1	**GAF**	67265	V20	48,0%	0,0%	100,0%	abnormal	Chromatin Structure/Topology
2	**Pita**	57732	V20	45,8%	0,0%	100,0%		Chromatin Structure/Topology
3	**HDAC3**	34778	V20	44,6%	0,0%	100,0%		Histone Acetylation
4	**nej**	homemade	V20	35,0%	0,0%	100,0%		Histone Acetylation
5	**E(z)**	33659	V20	32,5%	0,0%	100,0%		Polycomb group/H3K27me3
6	**CtBP**	32889	V20	31,7%	0,0%	100,0%		Chromatin Remodelling
7	**chm**	32484	V20	29,2%	0,0%	100,0%		Histone Acetylation
8	**Gug**	32961	V20	15,0%	0,0%	100,0%		Transcriptional Corepressor
9	**ZIP1C**	64552	V20	13,3%	0,0%	100,0%		Chromatin Structure/Topology
10	**domino**	41674	V20	11,1%	0,0%	100,0%	abnormal	Chromatin Remodelling
11	**Bre1**	35443	V22	9,0%	0,0%	100,0%	abnormal	Thritorax group/H3K4me3
12	**trr**	36916	V20	3,3%	0,0%	100,0%	abnormal	Thritorax group/H3K4me3
13	**Chd1**	34665	V20	2,9%	0,0%	100,0%	abnormal	Chromatin Remodelling
14	**egg**	32445	V20	2,5%	0,0%	100,0%		Heterochromatin/H3K9me3
15	**HDAC1**	33725	V20	51,3%	0,3%	99,5%		Histone Acetylation
16	**nurf38**	35444	V22	3,3%	0,4%	87,5%		Chromatin Remodelling
17	**Gcn5**	35601	V20	25,1%	3,9%	84,5%		Histone Acetylation
18	**Psc**	38261	V20	49,2%	7,8%	84,2%		Polycomb group/H3K27me3
19	**Hp1a**	36792	V22	43,6%	8,3%	80,9%		Heterochromatin/H3K9me3
20	**upSET**	51447	V20	43,3%	8,8%	79,8%	abnormal	Thritorax group/H3K4me3
21	**taf1**	32421	V20	22,7%	5,1%	77,6%	abnormal	Histone Acetylation
22	**csul**	56978	V20	63,3%	20,4%	67,8%		Arginine methyltransferase
23	**SMC2**	32369	V20	1,7%	0,6%	66,6%		Chromatin Structure/Topology
24	**DMAP1**	63666	V20	42,0%	14,2%	66,3%	abnormal	Chromatin Remodelling
25	**Scm**	55278	V20	24,0%	8,7%	63,9%		Polycomb group/H3K27me3
26	**msl-1**	39012	V20	23,3%	10,0%	57,1%		Histone Acetylation
27	**SMC5**	56035	V20	65,7%	29,4%	55,3%		Chromatin Structure/Topology
28	**bigH1**	34548	KK	35,0%	17,5%	50,0%		Chromatin Structure/Topology
29	**Chro**	57470	V20	95,0%	48,5%	49,0%		Chromatin Structure/Topology
30	**Mod(mdg4)**	32995	V20	0,8%	0,4%	47,9%	abnormal	Chromatin Structure/Topology
31	**ash2**	64942	V20	33,0%	17,6%	46,8%		Thritorax group/H3K4me3
32	**su(Hw)**	34006	V20	53,3%	28,7%	46,1%		Chromatin Structure/Topology
33	**dwg**	35666	V22	9,4%	5,3%	44,0%		Chromatin Structure/Topology
34	**kis**	34908	V20	87,5%	50,8%	42,0%		Chromatin Remodelling
35	**Pc**	36070	V22	24,2%	14,2%	41,5%		Polycomb group/H3K27me3
36	**Nap1**	35445	V22	65,0%	41,1%	36,8%		Chromatin Remodelling
37	**BRWD3**	33421	V20	45,6%	28,8%	36,7%		Histone Acetylation
38	**ash1**	36803	V22	60,0%	38,0%	36,7%		Thritorax group/H3K4me3
39	**Art3**	109448	KK	37,5%	24,4%	34,8%		Arginine methyltransferase
40	**calypso**	56888	V20	72,5%	47,9%	33,9%		Polycomb group/H3K27me3
41	**trx**	33703	V20	59,2%	39,6%	33,1%		Thritorax group/H3K4me3
42	**ear**	34798	V20	65,0%	44,2%	32,1%		Transcriptional Coactivator
43	**Sce**	35446	V22	35,8%	24,6%	31,4%		Polycomb group/H3K27me3
44	**enok**	41664	V20	36,3%	25,4%	29,9%		Histone Acetylation
45	**Sirt1**	32481	V20	57,5%	40,6%	29,5%		Histone Acetylation
46	**Set1**	33704	V20	26,7%	18,9%	29,2%	abnormal	Thritorax group/H3K4me3
47	**ttk**	36748	V20	80,0%	56,8%	29,0%		Chromatin Remodelling
48	**mof**	58281	V20	52,5%	37,5%	28,6%		Histone Acetylation
49	**Utx**	34076	V20	47,5%	34,4%	27,5%		Thritorax group/H3K4me3
50	**gro**	35759	V20	1,7%	1,3%	26,7%		Transcriptional Corepressor
51	**HDAC11**	32480	V20	46,3%	34,0%	26,6%		Histone Acetylation
52	**Brd8**	42658	V20	83,0%	61,0%	26,6%		Histone Acetylation
53	**Su(var)3-3**	32853	V20	61,0%	45,7%	25,1%		Heterochromatin/H3K9me3
54	**PR-Set7**	35322	V22	18,1%	13,7%	24,3%		Heterochromatin/H3K9me3
55	**gpp**	34842	V20	6,0%	4,6%	23,0%	abnormal	SET domain protein
56	**Ph**	63018	V20	70,8%	55,4%	21,8%		Polycomb group/H3K27me3
57	**Sin3A**	32368	V20	57,5%	45,0%	21,7%		Histone Acetylation
58	**Jarid2**	32891	V20	11,7%	9,2%	21,4%		Polycomb group/H3K27me3
59	**bbx**	57553	V20	75,8%	60,6%	20,1%		HMG box protein
60	**bon**	37515	V20	85,0%	68,3%	19,6%		Heterochromatin/H3K9me3
61	**SMC1**	108922	KK	26,7%	22,1%	17,2%		Chromatin Structure/Topology
62	**Hmt4-20**	32892	V20	76,6%	63,9%	16,6%		Heterochromatin/H3K9me3
63	**Ntmt**	110351	KK	92,0%	77,5%	15,8%		H2B methylation
64	**Sirt7**	32483	V20	73,5%	62,3%	15,2%		Histone Acetylation
65	**Smyd4-1**	106709	KK	87,5%	74,4%	14,9%		SET domain protein
66	**CoRest**	104900	KK	63,3%	54,2%	14,5%		Heterochromatin/H3K9me3
67	**Sox14**	34794	V20	92,5%	79,2%	14,4%		HMG box protein
68	**Art4**	36833	V22	83,3%	71,7%	14,0%	abnormal	Arginine methyltransferase
69	**top3**	108258	KK	76,7%	66,0%	13,9%	abnormal	Chromatin Structure/Topology
70	**ctcf**	40850	V20	62,5%	53,9%	13,8%		Chromatin Structure/Topology
71	**HmgD**	77429	V20	79,2%	68,3%	13,7%		Chromatin Structure/Topology
72	**HDAC6**	34072	V20	35,3%	30,6%	13,3%		Histone Acetylation
73	**G9a**	34817	V20	70,8%	61,7%	12,9%		Heterochromatin/H3K9me3
74	**Br140**	42502	V20	84,2%	73,3%	12,9%		Histone Acetylation
75	**Elba2**	61903	V20	94,2%	82,2%	12,7%		Chromatin Structure/Topology
76	**E(Pc)**	67921	V20	6,0%	5,3%	12,4%	abnormal	Chromatin Remodelling
77	**Acf**	35575	V22	80,8%	70,8%	12,4%		Chromatin Remodelling
78	**msl-2**	35390	V22	74,2%	65,0%	12,4%		Histone Acetylation
79	**Sirt4**	33984	V20	41,0%	36,0%	12,2%		Histone Acetylation
80	**HP1c**	33962	V20	92,5%	82,2%	11,1%		Heterochromatin/H3K9me3
81	**Ino80**	33708	V20	60,8%	54,2%	11,0%	abnormal	Chromatin Remodelling
82	**Iswi**	32845	V20	58,3%	52,1%	10,7%		Chromatin Remodelling
83	**Art8**	20307	GD	89,2%	80,3%	10,0%		Arginine methyltransferase
84	**Kdm4A**	34629	V20	85,0%	76,7%	9,8%		Heterochromatin/H3K9me3
85	**Kdm4B**	62409	V20	78,3%	70,8%	9,6%		Heterochromatin/H3K9me3
86	**dikar**	58280	V20	55,8%	51,1%	8,4%	abnormal	Histone Acetylation
87	**lid**	36652	V22	87,5%	80,6%	7,9%		Transcriptional Corepressor
88	**beaf32**	35642	V21	27,5%	25,4%	7,6%		Chromatin Structure/Topology
89	**NSD**	34033	V20	5,8%	5,4%	7,1%		SET domain protein
90	**Chd3**	33420	V20	58,3%	54,6%	6,4%		Chromatin Remodelling
91	**Art7**	36832	V22	80,8%	75,9%	6,1%		Arginine methyltransferase
92	**Atac2**	53918	V20	30,8%	29,2%	5,2%	abnormal	Histone Acetylation
93	**SuUR**	36893	V22	46,7%	44,3%	5,1%		Heterochromatin/H3K9me3
94	**Parp**	57265	V20	82,5%	78,3%	5,1%		Chromatin Structure/Topology
95	**dKDM2**	33699	V20	61,7%	58,6%	5,0%	abnormal	Polycomb group/H3K27me3
96	**JIL1**	55875	V20	62,5%	59,6%	4,7%		Kinase
97	**Sirt6**	34530	V20	48,1%	45,9%	4,5%		Histone Acetylation
98	**brm**	37721	GD	10,0%	9,6%	4,2%		Chromatin Remodelling
99	**Smyd5**	28609	V10	92,4%	88,6%	4,1%		SET domain protein
100	**l(3)mbt**	35052	V20	72,5%	69,6%	4,0%		Heterochromatin/H3K9me3
101	**Sirt2**	32482	V20	68,0%	65,3%	4,0%		Histone Acetylation
102	**HDAC4**	34774	V20	62,5%	60,0%	4,0%		Histone Acetylation
103	**set2**	42511	V20	87,8%	84,4%	3,9%		SET domain protein
104	**CP190**	33903	V20	43,3%	41,7%	3,8%		Chromatin Structure/Topology
105	**polybromo**	32840	V20	88,3%	85,0%	3,8%		Chromatin Remodelling
106	**MRG15**	35241	V22	95,8%	92,5%	3,5%		Histone Acetylation
107	**cic**	25995	V10	89,2%	86,4%	3,1%		HMG box protein
108	**tou**	35790	V22	77,0%	75,1%	2,5%		Chromatin Remodelling
109	**E(bx)**	33658	V20	35,8%	35,0%	2,3%		Chromatin Remodelling
110	**Hmg-2**	42542	V20	90,0%	88,3%	1,9%		HMG box protein
111	**Smyd4-4**	40705	GD	96,7%	95,0%	1,7%		SET domain protein
112	**CHRAC-16**	63658	V20	96,7%	95,3%	1,4%		Chromatin Remodelling
113	**CONTROL**	36303	-	98,3%	96,9%	1,4%		-
114	**rhi**	35171	V22	0,8%	0,8%	0,0%	abnormal	Heterochromatin/H3K9me3
115	**Cdk1**	36117	V20	0,0%	0,0%	0,0%	abnormal	Kinase
116	**fs(1)Ya**	64597	V20	0,0%	0,0%	0,0%		Histone Acetylation
117	**Top2**	35416	V22	0,0%	0,0%	0,0%		Chromatin Structure/Topology
118	**scrawny**	40865	V20	-	-	-	no eggs	Thritorax group/H3K4me3
119	**Tlk**	33983	V20	-	-	-	no eggs	Kinase
120	**fs(1)h**	35139	V22	-	-	-	no eggs	Histone Acetylation
121	**Mi-2**	33419	V20	-	-	-	no eggs	Chromatin Remodelling
122	**Sfmbt**	32473	V20	-	-	-	no eggs	Polycomb group/H3K27me3
123	**Top1**	55314	V20	-	-	-	no eggs	Chromatin Structure/Topology
124	**D12**	65062	V20	-	-	-	no eggs	Histone Acetylation
125	**piwi**	33724	V20	-	-	-	no eggs	Heterochromatin/H3K9me3
126	**dre4**	41677	V20	-	-	-	no eggs	Chromatin Remodelling
127	**Ssrp**	41719	V20	-	-	-	no eggs	Chromatin Remodelling

Table S2. List of antibodies used in this work

Antigen	Antibody name	Host	Source
H3K9ac	H3K9ac - EpiCypher SNAP-ChIP	Rabbit monoclonal	EpiCypher (BioCat)
H3K18ac	Histone H3K18ac antibody (pAb)	Rabbit polyclonal	Active Motif
H3K27ac	Anti-acetyl Histone H3(Lys27) (Clone No MABI0309)	Mouse monoclonal	Wako
H3K23ac	Histone H3K23ac antibody (pAb)	Rabbit polyclonal	Active Motif
H3	Histone H3 Antibody (ChIP Formulated)	Rabbit polyclonal	Cell Signaling
H4	HRP Anti-Histone H4 antibody [mAbcam 31830]	Mouse monoclonal	Abcam
Nejire	anti-CBP	Rabbit polyclonal	Nadezhda E. Vorobyeva (homemade)
Gcn5	anti-Gcn5	Rabbit polyclonal	Aleksey N. Krasnov (homemade)
GAF	anti-GAF	Rabbit polyclonal	Maxim Erokhin and Daria Chetverina (homemade)
Zelda	rZld	Rabbit polyclonal	Melissa M. Harrison (homemade)
HA	Anti-HA.11 Epitope Tag Antibody	Mouse monoclonal	Covance
rabbit IgG (H+L)	F(ab')2-Goat anti-Rabbit IgG (H+L) Cross-Adsorbed Secondary Antibody, Alexa Fluor™ 488	Goat polyclonal	Molecular Probes by ThermoScientific
mouse IgG (H+L)	F(ab')2-Goat anti-Mouse IgG (H+L) Cross-Adsorbed Secondary Antibody, Alexa Fluor™ 555	Goat polyclonal	Molecular Probes by ThermoScientific

Antigen	Catalog number or reference	Lot number	conc. used for IF	conc. used for WB	quantity for Cut&Tag
H3K9ac	13-0033	19091001	1 to 200	1 to 1000	1µg
H3K18ac	39587	7909001	1 to 200	1 to 5000	1µg
H3K27ac	306-34849	11003	1 to 100	1 to 1000	1µg
H3K23ac	39131	1008001	1 to 200	-	1µg
H3	#2650	4	-	-	1µg
H4	ab197517	GR3357384-5	-	1 to 1000	-
Nejire	https://www.sciencedirect.com/science/article/pii/S1874939917302924	-	1 to 200	1 to 500	-
Gcn5	https://academic.oup.com/nar/article/41/11/5717/2411603	-	1 to 200	1 to 500	1µg
GAF	https://www.pnas.org/doi/10.1073/pnas.1515276112	-	1 to 100	1 to 200	-
Zelda	https://doi.org/10.1016/j.ydbio.2010.06.026	-	1 to 200	1 to 200	-
HA	MMS101R	B224726	-	-	1µg
rabbit IgG (H+L)	A11070	1775509	1 to 500	-	-
mouse IgG (H+L)	A21425	1874003A	1 to 500	-	-